Fluid Self-Diffusion in Scots Pine Sapwood Tracheid Cells

ARTICLE *in* THE JOURNAL OF PHYSICAL CHEMISTRY B · MARCH 2006

Impact Factor: 3.3 · DOI: 10.1021/jp055643l · Source: PubMed

3 AUTHORS:

Espen Johannessen
Narvik University College
12 PUBLICATIONS **97** CITATIONS
SEE PROFILE

Eddy Walther. Hansen
University of Oslo
112 PUBLICATIONS **1,474** CITATIONS
SEE PROFILE

Jarl B. Rosenholm
Åbo Akademi University
272 PUBLICATIONS **3,068** CITATIONS
SEE PROFILE

Fluid Self-Diffusion in Scots Pine Sapwood Tracheid Cells

Espen H. Johannessen,*,† Eddy W. Hansen,‡ and Jarl B. Rosenholm*,†

Graduate School of Materials Research, Department of Physical Chemistry, Åbo Akademi University, Porthansgatan 3-5, FI-20500 Turku, Finland, and Department of Chemistry, University of Oslo, P.O. Box 1033 Blindern, NO-0315 Oslo, Norway

Received: October 4, 2005; In Final Form: November 30, 2005

The self-diffusion coefficients of water and toluene in Scots pine sapwood was measured using low field pulsed field gradient nuclear magnetic resonance (PFG-NMR). Wood chips of 8 mm diameter were saturated with the respective liquids, and liquid self-diffusion was then traced in one dimension orthogonal to the tracheid cell walls in the wood's radial direction. The experimental echo attenuation curves were exponential, and characteristic self-diffusion coefficients were produced for diffusion times spanning from very short times to times on the order of magnitude of seconds. Observed self-diffusion coefficients were decaying asymptotically as a function of diffusion time, an effect which was ascribed to the cell walls' restriction on confined liquid diffusion. The observed self-diffusion behavior in Scots pine sapwood was compared to self-diffusion coefficients obtained from simulations of diffusion in a square. Principles of molecular displacements in confined geometries were used for elucidating the wood's cellular structure from the observed diffusion coefficients. The results were compared with a mathematical model for diffusion between parallel planes.

Introduction

The study of self-diffusion in biological tissue is an area of research with high activity. Specific attention in this field concerns the application of self-diffusion studies in white matter in the brain.[1] The present work presents the self-diffusion behavior in Scots pine sapwood tracheid cells. As a matter of fact, the cellular structure of sapwood and brain white matter is very similar. Scots pine sapwood consists of more than 90% tracheid cells. These cells have hollow cavities or lumens. Tracheid cells of average length are just below 3 mm, while the cross-sectional diameter varies from 20 to 30 μm. The wood matrix thus resembles an anisotropic structure with two-dimensional symmetry. The cross-sectional shape of the cells is either squarelike or circlelike. For Scots pine, the shape tends to be more squarelike.[2] Diffusion of liquids confined in the cell lumens is, thus, free in the direction parallel to the cell lengths and is affected by the cell wall restriction orthogonal to the cell lengths, as observed on the pulsed field gradient nuclear magnetic resonance (PFG-NMR) time scale. This is visualized in Figure 1. The tracheid cell walls have pits distributed along the cell lengths. These pits are covered with a membrane much thinner than the rest of the cell wall. The obvious function of the pits is to allow for intercellular liquid diffusion and, thereby, regulate liquid transport processes in the tree. One goal of this work is to see if intercellular self-diffusion can be observed when the system is at equilibrium.

Earlier PFG-NMR studies of biological systems focus on for instance wood pulp fibers and potato starch granules,[3] wet cotton,[4] cell suspensions,[5,6] and liposomes.[7,8]

Wood is a natural material possessing cell size distribution, chemical extractives, and physicochemical interactions with cell confined liquids. With this fact in mind, two different liquids

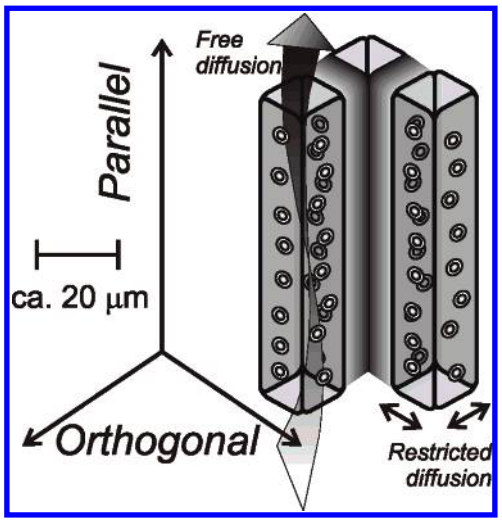

Figure 1. Principal structure of tracheid cells. The two anisotropic self-diffusion paths are shown. Diffusion parallel to the cell lengths is free, while diffusion orthogonal to the cell lengths is restricted by the cell walls.

of highly different properties were selected as cell structure tracing fluids. The water transporting features of the tracheid cell lumen is based to a high degree on hydroxyl groups in cellulose and, thereby, on polar interactions between the cell wall and the confined water. The polarity of the confined molecules can be classified according to their Lewis basicity and acidity through donor numbers (DN) and acceptor numbers (AN), respectively. The water molecule is a typical dipole and has $(DN + AN)^{1/2} = 8.44$. Toluene on the other hand is a very weak base where the π-electrons in the benzene ring give rise to the basicity, and toluene has $(DN + AN)^{1/2} = 0.95$.[9,10]

Experimental Details

PFG-NMR. Scots pine, *Pinus sylvestris*, was harvested in Finland, and in the greenwood state, sapwood from one and

* Corresponding authors. E-mail: espen@vistacell.com. Telephone: +358 2215 4616. Fax: +358 2215 4706.
† Åbo Akademi University.
‡ University of Oslo.

10.1021/jp055643l CCC: $33.50
Published on Web 01/12/2006

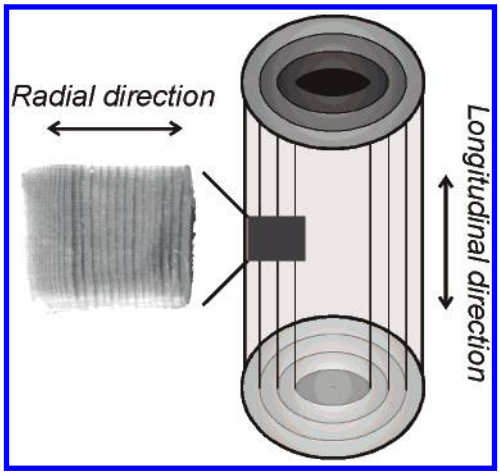

Figure 2. Sketch of a wood stem. The wood's tracheid cells create fibers on the order of a millimeter in length in the longitudinal direction. In the radial direction, the cells have diameters on the order of micrometers. The sample plugs were created by drilling from a tangential cut under the bark toward the stem center in the radial direction.

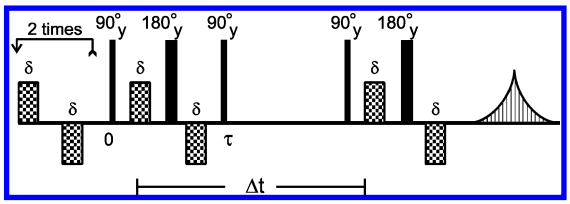

Figure 3. Diagram visualizing the events through the PFGSTE pulse sequence. The gradient pulses are symbolized with checked boxes. Positive gradient pulses point upward from the time line, while negative gradient pulses point downward. All gradient pulses are applied over time δ. Radio frequent pulses are symbolized with tall black bars. The actual manipulation of the molecule population starts at time 0 and ends with the detection of the echo magnitude at the end of the time span. The molecular self-diffusion is traced during the diffusion time, Δt. The preparatory gradient pulses were used for stabilizing the output from the gradient power supply before starting the actual diffusion experiment.

the same tree was used as the origin for cylindrical chips of 8 mm in diameter and approximately 10 mm in length created with a plug drill. Figure 2 shows a cartoon of the sample plug's orientation[11] relative to the wood stem.

The freshly prepared plugs were either saturated with distilled water, H_2O, or gently dried and saturated with toluene, C_7H_8. In both cases, the wood chips were floating in the liquid in a low-pressure atmosphere. They were then left to absorb the surrounding liquid until the wood chips' density equaled the respective liquids' density and no more bubbles were escaping from the chips. After this simple preparation, the chips were wiped and inserted into NMR tubes of 10 mm outer diameter. A vortex plug was placed on top of the sample chip in the tube to prevent evaporation. The PFG-NMR diffusion experiments were performed with a benchtop NMR instrument of the type Maran Ultra from Resonance Instruments. The instrument was sending and receiving the ^{1}H nuclide at 23 MHz. During all experiments, the sample temperature was set to 30 °C. According to NMR principles, the self-diffusion coefficient of the confined liquid was measured with a pulsed field gradient stimulated echo (PFGSTE) pulse sequence. To optimize the instruments performance and maximize the experimental credibility, a pulse sequence optimized for low field benchtop systems with permanent magnets was used. The utilized pulse sequence is envisaged in Figure 3. The pulse sequence also suppresses the effects of cross relaxation between the confined

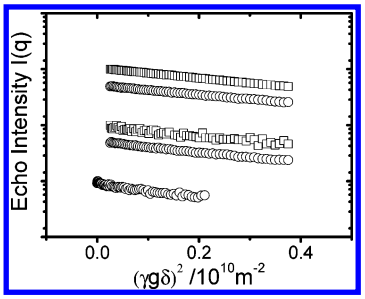

Figure 4. Echo attenuation curves at two different diffusion times for water (squares) and at three different diffusion times for toluene (circles). The intensities are plotted in arbitrary units semilogarithmically as a function of $(\gamma g\delta)^2$. The two upper curves represent a 100 ms diffusion time, the two middle ones represent a 500 ms diffusion time, and the lower curve represents a 3000 ms diffusion time.

liquid and the cell wall,[12] a phenomenon which indeed exists in wood.[13]

During the PFGSTE experiment, molecular displacement is traced using a magnetic gradient. The gradient is applied with strength g and in pulses of length δ, thus giving a resonance frequency which depends on the spatial position at the x-axis. The molecular population is thus tagged during the gradient pulses if their spin vectors are in the yz-plane at that moment. Utilizing the signal attenuation that occurs between pairs of gradient pulses, the average mean squared displacement of the molecular population can be obtained. As a matter of fact, the echo intensity detected at the end of the diffusion experiment is given as an exponential function when the diffusion propagator is Gaussian:

$$\frac{I}{I_0} = \exp\left[-4(\gamma g\delta)^2 D\left(\Delta t + \frac{3}{2}\tau - \frac{\delta}{2}\right)\right] \qquad (1)$$

where D is the observed molecules' self-diffusion coefficient, γ is the gyromagnetic ratio for ^{1}H, g is the magnetic field gradient strength during pulses of length δ, Δt is the diffusion time, and τ is the time of a tagging block in the pulse sequence. By acquiring the signal intensity for variable g, the self-diffusion coefficients, D, of water and toluene were calculated from the slope of the attenuation curves. Such experiments were done for different diffusion times, Δt. The pulse length, δ, was kept constant at 0.5 ms, and the gradient strength, g, was varied from 0 up to 1.15 T m^{-1} for the experiment with $\Delta t = 10$ ms and up to 0.34 T m^{-1} for the experiment with $\Delta t = 3000$ ms. In principle, echo attenuation curves exhibit nonexponential behavior when the observed molecules' self-diffusion is hindered.[14] The initial slope of the curve will, though, represent the molecular population's mean square displacement also for restricted diffusion.[15] Only exponential echo attenuation curves were observed in this work, something that means that the diffusion restriction effect was not affecting the shape of the attenuation curves observed with the given setup. It should also be emphasized that the applied pulse sequence is optimized for the low field NMR instrument used by effectively hindering eddy currents from producing artifacts in the acquired data. Figure 4 shows echo attenuation curves for different arbitrary diffusion times representing PFG-NMR experiments of both water and toluene diffusion in wood. The intrinsic self-diffusion coefficients of water and, respectively, toluene were measured to be 2.1×10^{-9} m^2 s^{-1} and 1.9×10^{-9} m^2 s^{-1} in bulk samples.

Dvinskikh and Furó have showed that effective cross relaxation affecting the observed species in an ordinary PFGSTE experiment results in a double-exponential curve when the signal intensity is plotted as a function of diffusion time, Δt.[12] The

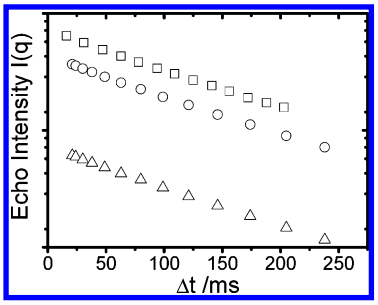

Figure 5. Echo attenuation curves from diffusion experiments on water confined in wood. The signal intensity is plotted semilogarithmically as a function of Δt. The same setup was used as for the experiments with variable gradient strength. For the squares g was 0.011 T m^{-1}, for the circles g was 0.069 T m^{-1}, and for the triangles g was 0.115 T m^{-1}. The exponential shapes of the plots are evidence of suppression of cross relaxation between water and the wood's solid matrix.

effect of cross relaxation is suppressed by utilizing the pulse sequence used in the present work. This can be confirmed by checking for exponential dependence between the signal intensity and the diffusion time. As seen in Figure 5, this was confirmed for experiments of diffusion of confined water in wood. Water is believed to have considerable interactions with the hydroxyl rich wood matrix.[13]

Self-Diffusion Modeling. A slice cut through a wood stem creates a cross-sectional view of the tracheid cells. The cross-sectional structure of a Scots pine tracheid cell is close to the shape of a square with a degree of curvature of the corners. The two-dimensional (2D) radial wood matrix constitution can thus be seen as an array of cells having idealized geometries close to the shapes of squares. For comparison with the experimentally obtained self-diffusion coefficients, 2D diffusion was modeled in squares. Discretization of the diffusion equation was done exploiting the finite element method through the software program COMSOL Multiphysics 3.2. Considering the diffusion in one dimension, the displacement of mass was described by Fick about 150 years ago:[16]

$$\frac{\partial c(x,\Delta t)}{\partial \Delta t} = D\frac{\partial^2 c(x,\Delta t)}{\partial x^2} \tag{2}$$

which is a partial differential equation. Equation 2 is numerically solved within COMSOL Multiphysics, something which allows the simulation of diffusion of a species with any given initial distribution. The modeling followed the principles outlined by Hagslätt and others.[17] A square was drawn with given dimensions and then partitioned into a number of elements, typically thousands. The simulation cell boundaries were defined as reflecting walls. For a liquid saturated porous sample at thermodynamic equilibrium, there are no macroscopic chemical gradients and, thus, no net movement of any chemical species. The PFG-NMR experiment labels molecules according to their spatial position on the x-axis and measures the molecular mean squared displacement along the x-axis. Principally, the sample then is an infinite number of stacked slices from which the diffusion is measured. The acquired signal represents a sum over all the slices. The starting position for slice i in the simulations was defined as

$$x_{0,i} = 1 + 2(i-1) \quad \text{for } 1 \le i \le 8 \tag{3}$$

The start time of the simulations was set to $\Delta t_{\min} = 1$ ms in order to give the labeled molecules originating from a given slice a continuous start distribution. The molecular distribution next to a straight wall is at the start time given by[18]

$$c(x,\Delta t_{\min};x_{0,i}) = \frac{M(x_{0,i},0)}{\sqrt{4\pi D_0 \Delta t_{\min}}}\left[\exp\left(-\frac{(x-x_{0,i}-a)^2}{4D_0\Delta t_{\min}}\right) + p\exp\left(-\frac{(x+x_{0,i}-a)^2}{4D_0\Delta t_{\min}}\right)\right] \tag{4}$$

where a is the distance from the box's midline to the wall, $x_{0,i}$ is the distance from slice i to the wall, $M(x_{0,i})$ is an arbitrarily initial density of molecules, and D_0 is the molecule's self-diffusion coefficient in the case of free diffusion. The term p is for a reflecting wall equal to 1 and equal to -1 in the case of an absorbing wall.

In Figure 6 is shown the start distribution of the sum of species 1 and 8 having start positions $x_{0,1} = 1$ μm and $x_{0,8} = 15$ μm, respectively.

Figure 6 reveals how the concentration distributions of position dependent slices vary according to the slice's distance from the surrounding walls. The molecules from the slice originating in the middle of the box are, at the start time, unaffected by the walls, and their molecular distribution is, as such, Gaussian. The molecules from the slice with a start position 1 μm from the wall, on the other hand, have at the start time a distribution clearly affected by the wall. The latter is reflected in a non-Gaussian molecular distribution for that slice. As diffusion time evolves, the slice dependent molecular distributions propagate differently. Each slice has its own distribution profile at every time step resulting from the simulations. This allows for calculation of the mean square displacement for molecules originating from every slice. The mean square displacement is given by the integral over x of the diffusion propagator, $P(x,t;x_{0,i})$, times the initial molecular density, $M(x_{0,i},0)$, times the displacement squared, $(x - x_{0,i})^2$,

$$\langle (x-x_{0,i})^2\rangle = \int_{\text{cell}} (x-x_{0,i})^2 M(x_{0,i},0)\, P(x,\Delta t;x_{0,i})\, \mathrm{d}x \tag{5}$$

In the simulations, all molecules are restricted by the cell walls and the density of molecules from one slice inside the cell will, thus, remain constant. This allows for

$$M(x_{0,i},0) = \int_{\text{cell}} c(x,\Delta t;x_{0,i})\, \mathrm{d}x \tag{6}$$

at all times. The propagator for molecules starting at position $x_{0,i}$ can for a selected time be calculated according to

$$P(x,\Delta t;x_{0,i}) = \frac{c(x,\Delta t;x_{0,i})}{\int_{\text{cell}} c(x,\Delta t_{\min};x_{0,i})\, \mathrm{d}x} \tag{7}$$

The mean-square displacement of molecules from slice i is

$$\langle (x-x_{0,i})^2\rangle = \frac{\int c(x,\Delta t;x_{0,i})(x-x_{0,i})^2\, \mathrm{d}x}{\int c(x;x_{0,i})\, \mathrm{d}x} \tag{8}$$

which was readily calculated for all eight slices in the simulations at every diffusion time step. Considering that the PFG-NMR method produces the mean-square displacement of the whole molecular population and, thereby, the system's self-diffusion coefficient, it was sought to calculate the total population's mean-square displacement from the diffusion simulations of the eight slices.

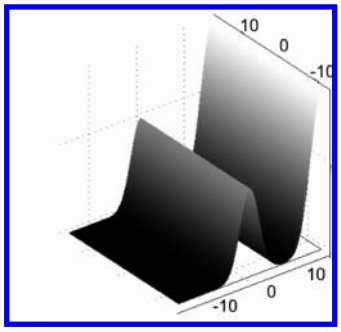

Figure 6. Distribution of species 1 ($x_{0,1} = 1\ \mu$m) and 8 ($x_{0,8} = 15\ \mu$m) in a box of width 30 μm at simulation start time 1 ms, according to eq 4. It is clearly seen how the distribution from the slice near the wall is the sum of a Gaussian distribution and its mirror image across the wall.

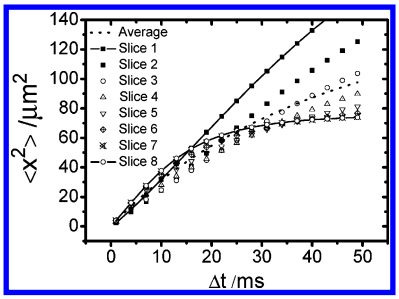

Figure 7. Mean-square displacement for the eight slices calculated from the simulations according to eq 8. Also is shown the total population approximation from a weight averaging of the eight slices.

Results and Discussion

In Figure 7 is shown the mean-square displacements calculated with eq 8 for the eight simulated slices, which have start positions from 1 μm from the wall for slice 1 to 15 μm from the wall for slice 8 which is on the cell's middle line. Note how the behavior is different relative to the slices' start positions. Molecules starting close to the wall (slice 1) have at first shorter displacement relative to the slices toward the cell center due to the fact that almost half of the molecules instantly collide with the wall. Reflection of the molecules by the wall creates a throng next to the wall. This leads to an increased possibility of the slice 1 labeled molecules diffusing from the wall toward the other side of the cell. Their mean-square displacement increase as a function of diffusion time is, thereby, more pronounced than for the molecules originating from the cell's midline. In fact, the mean-square displacement of slice 1 molecules crosses the that of the slice 8 molecules at about 16 ms of diffusion time. Slice 8's molecules originate from the middle of the cell, and on average, half of its molecules will diffuse toward the left and half of its molecules will diffuse toward the right. The distances to both the walls are the same from slice 8. At the lowest diffusion times, the diffusion from slice 8 is free because no molecules from the slice have collided with the sidewalls. As noted from Figure 7, the middle slice's mean-square displacement also is higher at the lower diffusion times relative to slice 1. Then, as diffusion time increases, molecules from slice 8 diffuse with equal probability toward both walls. Restriction from both the walls will thus influence the mean-square displacement of slice 8, and it has a relatively faster decrease in mean-square displacement as diffusion time steps forward. Generally, each slice has a mean-square displacement sigmoid curve with diffusion time at the abscissa. As previously stated, PFG-NMR does not produce slice specific diffusion propagators but a total population diffusion propagator. The total population mean-square displacement of the simulated system was thus estimated through

$$\langle (x - x_0)^2 \rangle_{\text{tot}} = \sum_i \frac{(x - x_{0,i})^2 M(x_{0,i},0)}{\sum_i M(x_{0,i},0)} \tag{9}$$

and is shown as a line in Figure 7. For about 100 years, the theory behind Brownian motion has been clear.[19] The mean-square displacement for free diffusion is given by 2 times the intrinsic self-diffusion coefficient times the diffusion time:

$$\langle (x(\Delta t) - x_0)^2 \rangle_{\text{free}} = 2D_0\Delta t \tag{10}$$

As explained above, the diffusion of all the molecules inside a cell is not free. Dependent on their start position and the diffusion time, a fraction of the molecules will bump into the sidewalls and experience the restriction of the walls.[20] If S is the total surface area of the walls restricting the molecular diffusion, then the volume of molecules that have "seen" the walls is $S(2D_0\Delta t)^{1/2}$. Taking the total cell volume as V, the fraction of restricted molecules is $[S(2D_0\Delta t)^{1/2}]/V$, and the fraction of unrestricted molecules is $1 - [S(2D_0\Delta t)^{1/2}]/V$. The mean-square displacement of the total molecular population is then

$$\langle (x(\Delta t) - x_0) \rangle_{\text{tot}} = \left(1 - \frac{S}{V}(2D_0\Delta t)^{1/2}\right)2D_0\Delta t + \text{constant} \times \frac{S}{V}(2D_0\Delta t)^{1/2}2D_0\Delta t \tag{11}$$

where a constant between 0 and 1 is used. The molecular displacement in a square cell parallel to two walls and orthogonal to the other two walls does, thus, "feel" the restriction of two of the walls. The aggregate length of these two walls is $2 \times 2a = 4a$, and the cross-sectional area of the cell is $(2a)^2 = 4a^2$. The apparent surface-to-volume ratio is, thus, connected to the cell side half length through $S/V = 4a/4a^2 = 1/a$.

Considering the actual mean-square displacements in Figure 7, there can be calculated apparent self-diffusion coefficients according to the principles of eq 10. Instead of the intrinsic self-diffusion coefficient, one must define the apparent self-diffusion coefficient for slice i as

$$D_i(\Delta t) = \frac{\langle (x(\Delta t) - x_{0,i})^2 \rangle}{2\Delta t} \tag{12}$$

which is a function of the diffusion time. The apparent self-diffusion coefficient of the molecules in question can, thus, be found from half the value of the slope of the mean-square displacement curve as a function of the diffusion time. The latter are revealed in Figure 8.

Figure 8 reflects well how the start position dependent behavior of the diffusion gives time variable slopes to the mean-square displacement curves. Molecules from slice 1 at first create a throng next to one of the walls and from there have an increasing, apparent self-diffusion coefficient until it reaches a maximum value at the instance when restriction of the other wall influences the diffusion. Molecules from slice 8 are, on the other hand, at first under no restriction by the walls and have an apparent self-diffusion coefficient equal to the intrinsic self-diffusion coefficient. As diffusion time increases, the apparent self-diffusion coefficient decreases due to restriction effects on the midplane molecules from both the walls. Note how the estimated total population apparent self-diffusion coefficient decreases linearly with the square root of the diffusion time. This is explained from known theory. The mean-

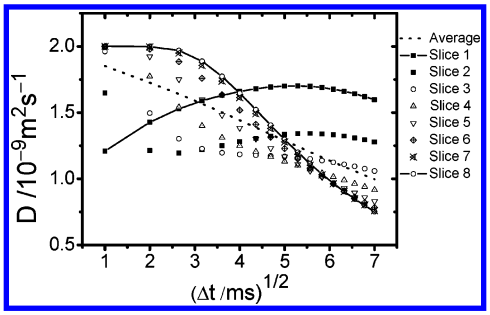

Figure 8. Apparent self-diffusion coefficients of the slice-dependent molecules calculated from simulations. The abscissa is represented by the square root of the diffusion time. Also, the estimated apparent self-diffusion coefficients of the whole population are shown.

square displacement of all the molecules in the cell is calculated by integrating eq 5 over all possible start positions:

$$\langle (x - x_0)^2 \rangle_{\text{tot}} = \int_{\text{cell}} \int (x - x_0)^2 M(x,0)\, P(x,\Delta t; x_0)\, \mathrm{d}x\, \mathrm{d}x_0 \tag{13}$$

Solving eq 13 for short times as shown by Mitra and others[21] reveals

$$D_{\text{tot}}(\Delta t) = D_0\left[1 - \frac{4S\sqrt{D_0 \Delta t}}{3V\sqrt{\pi}}\right] \tag{14}$$

The linear decrease in the apparent self-diffusion coefficient verses the square root of the diffusion time is, thus, the expected behavior considering the whole population.

The above statement is evidently true at shorter diffusion times. At longer diffusion times though, the mean-square displacement of all molecules will be upward limited by the walls and, as such, will reach an asymptotic value. Thus, when $2a$ is the width of the confining cell, $\langle (x(t) - x_0)^2 \rangle_{\text{tot}} \rightarrow$ constant $\times (2a)^2$. The literal explanation of this is that the molecules will loose the memory of their initial positions at long diffusion times, and final positions will be uniformly distributed. Considering eq 13, the propagator is then equal to $M(x_0,0)$ for all positions, and the initial molecular density is 1/(2a). So $\langle (x(\Delta t \rightarrow \infty) - x_0)^2 \rangle_{\text{tot}}$ is given by the length integral over the initial and final positions,

$$\langle (x(\Delta t \rightarrow \infty) - x_0)^2 \rangle_{\text{tot}} = \frac{\int_{\text{cell}} \int (x - x_0)^2\, \mathrm{d}x\, \mathrm{d}x_0}{(2a)^2} = \frac{2}{3}a^2 \tag{15}$$

and is, thus, independent of the intrinsic self-diffusion coefficient of the molecules. The apparent self-diffusion coefficient at long times is thus

$$D_{\text{tot}}(\Delta t \rightarrow \infty) = \frac{a^2}{3\Delta t} \tag{16}$$

Note that eq 16 has 3 in the denominator due to the square shaped cell.

Generally, intercellular diffusion occurs in biological tissue, and wood is no exception to this. For example, water lifting in trees requires[22] extensive intercellular diffusion, while other compounds such as nutrients have different diffusion paths. In connected cellular systems, the apparent self-diffusion coefficient will reach a value higher than zero. This is the effective self-diffusion coefficient of the system:

$$D_\infty = D(\Delta t \rightarrow \infty) \rightarrow \frac{D_0}{\alpha} \tag{17}$$

where α is a dimensionless factor defining the systems tortuosity. It is interesting to note how the apparent self-diffusion coefficient approaches the effective self-diffusion coefficient. Figure 9 shows how simulations of diffusion in a square cell reveal mean-square displacements which approach an asymptotic level dependent on the start positions for long diffusion times. The asymptotic levels of the mean-square displacements are in agreement with eq 15 and confirm that D_∞ is zero regardless of start position for a geometrically closed cell. In the case of impenetrable walls, α, thus, reaches infinity and the effective self-diffusion coefficient becomes zero.

Cell Structure Elucidation. It is now clear that the diffusion behaves differently at short diffusion times relative to long diffusion times. These two different behaviors and the connection between them can be used to interpret structural properties of the material. Equation 14 expresses the ratio between the internal surface and the pore volume of the material S/V. When the apparent self-diffusion coefficients follow the trend of proportionality to the square-root of diffusion time, they can be fitted to the equation through least-squares's curve fitting and output the surface-to-volume ratio. Fitting of the obtained apparent self-diffusion coefficients from diffusion simulation in the 30 μm wide square cell and the PFG-NMR diffusion experiments at short diffusion times is shown in Figure 10 for diffusion times from 1 to 40 ms.

The obtained surface-to-volume ratio for the simulated cell was $S/V = 0.0664\ \mu\text{m}^{-1}$ which by inversion gives the cell side half length as $a = 15.06\ \mu$m. This is in agreement with the cell's real size in COMSOL Multiphysics, where the side length was set to 30 μm. Fitting the experimentally obtained self-diffusion coefficients gave almost identical cell side half lengths. For toluene, the value $a = 10.8\ \mu$m was obtained, while for water the result was $a = 10.9\ \mu$m.

Proceeding to long diffusion times, the behavior of the apparent self-diffusion coefficients turns to follow proportionality to diffusion time inversed. The apparent self-diffusion coefficients obtained by simulation were fitted to eq 16 for diffusion times between 500 and 2000 ms. Similarly, the observed self-diffusion coefficients for toluene between 1000 and 3000 ms of diffusion time were fitted to the same equation. Both fittings are shown in Figure 11.

Optimizing the unknown cell size through the fit gave $a = 14.75\ \mu$m for the simulated self-diffusion coefficients. This is, thus, a small deviation from the value of a used for the simulation cell in COMSOL Multiphysics, which was 15 μm. The deviation is due to the fact that short diffusion time behavior still affects the data to some degree. The fitting to observed self-diffusion coefficients for toluene gave $a = 13.5\ (\pm 1)\ \mu$m but depended upon what was selected as the shortest time in the fitting procedure.

An important step in the progress in interpretation of time-dependent diffusion coefficients was the introduction of Padé approximants for interpolation of short diffusion time and long diffusion time data.[23] With this method, the self-diffusion coefficient behavior at all diffusion times is described as

$$D(\Delta t) = D_0\left[\frac{1}{1 + \frac{4S}{3\sqrt{\pi}V}\sqrt{D_0 \Delta t} + \frac{\Delta t}{\theta}}\right] \tag{18}$$

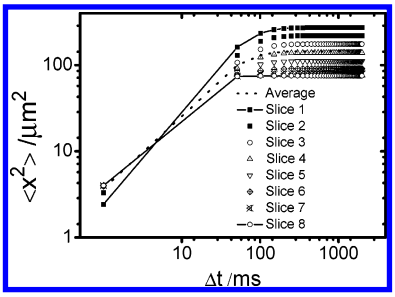

Figure 9. Mean-square displacements of simulated diffusion in a square cell with variable start positions. The long time behavior of the mean-square displacements is an asymptotic approach to levels determined by the cell wall restrictions. The reader should note that the total population's long time mean-square displacement level is a result of averaging all the slices' asymptotic levels.

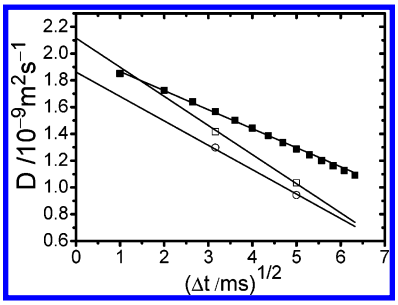

Figure 10. Apparent self-diffusion coefficients obtained by simulation (filled squares), measurements of water diffusion (open squares), and measurements of toluene diffusion (circles). Least-squares fitting of eq 14 to the values resulted in the lines.

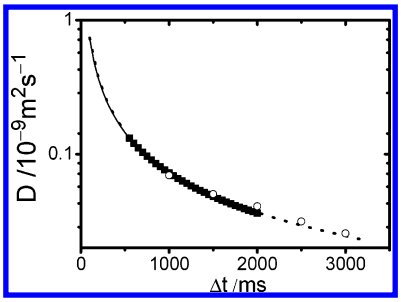

Figure 11. Apparent self-diffusion coefficients for long diffusion times. Filled squares correspond to simulations and open circles correspond to measured toluene diffusion. Fits to eq 16 are shown by the solid line for the simulated data and the dotted line for toluene diffusion.

when no intercellular diffusion occurs. The parameter θ is a characteristic time for the diffusion behavior in the material. Data of all diffusion times were fitted to eq 18. During the fitting processes, the characteristic time, θ, and the surface-to-volume ratio, S/V, were both optimized freely. The resulting fits are shown in Figure 12 for the simulated self-diffusion coefficients and in Figure 13 for the experimental diffusion of toluene and water in wood.

The fitting result of simulated diffusion gave a characteristic time, θ, equal to 56.28 ms. This is the time needed for all of the molecules to experience the cell's surroundings. From this, a characteristic size of the cell was found which was in perfect agreement with the cell side half length through $(2D_0\theta)^{1/2} = 15.00 = a$.

The optimized parameters resulting from the fittings are shown in Table 1. Note that the real surface-to-volume ratio of the trachid cell lumens is given by doubling the reported S/V. This is due to the fact that only the cell sides orthogonal to the diffusion direction contribute to the obtained values.

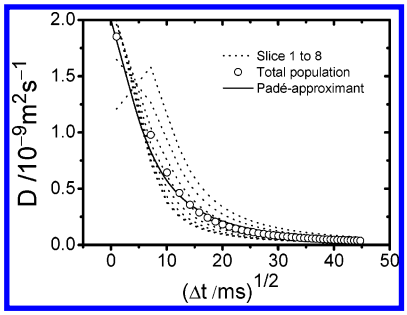

Figure 12. Apparent self-diffusion coefficients at all diffusion times obtained by simulation. The line is a fit to the Padé approximant, eq 18.

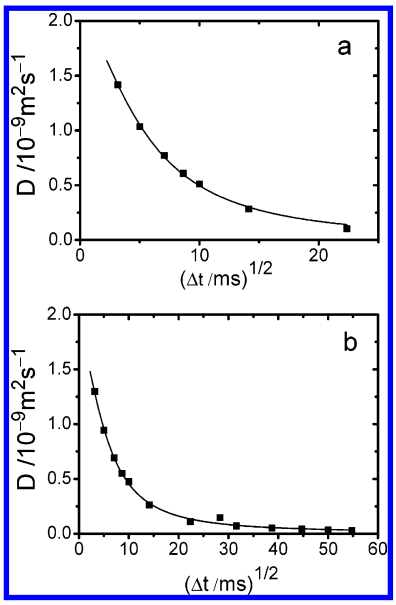

Figure 13. Observed self-diffusion coefficients of water (a) and toluene (b) confined in wood. The lines are fits to eq 18.

TABLE 1. Parameters Obtained from Fitting Observed Self-diffusion Coefficients of Confined Water and Toluene in Scots Pine Sapwood[a]

	S/V (μm^{-1})	$a = 1/(S/V)$ (μm)	θ (ms)	$(2D_0\theta)^{1/2}$ (μm)
water	0.078	12.9	40.3	13.0
toluene	0.068	14.7	39.5	12.3

[a] Note that the reported S/Vs only reflect two of the cell walls. "Real" S/Vs are thus obtained by doubling the reported values.

The fact that the long time effective self-diffusion coefficient was measured to be zero (see eq 17), with both liquids, showed that the diffusion in the cell lumens was fully restricted by the walls and no significant intercellular diffusion could be observed. Thus, eq 18 is also valid for the real wood systems. This raises the question of whether the diffusion in the system can be described analytically as diffusion between parallel walls. Frey and others[18] showed (with the basis in eq 4) that the apparent self-diffusion coefficient of liquids confined between parallel walls is given analytically as

$$D(t') = D_0\left[\frac{1}{\psi_0 2t'}\left[\frac{1+p}{12} - \frac{2}{\pi^4}\sum_{k=1}^{\infty} \times \frac{\exp(-\pi^2 k^2 t')}{k^4}((-1)^k\pi^2k^2(1-p) + (1-(-1)^k)(6-2p))\right]\right] \quad (19)$$

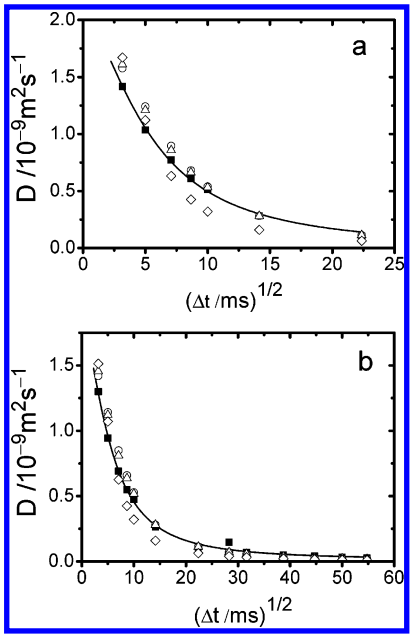

Figure 14. Comparison of the experimentally observed self-diffusion coefficients (filled squares) and the Padé approximant (line) with self-diffusion coefficients calculated according to eq 19 with $a = 13$ μm, $p = 1$ (circles), $p = 0$ (triangles), and $p = -1$ (diamonds). Part a corresponds to the diffusion of water, and part b corresponds to the diffusion of toluene.

with the normalized diffusion time

$$t' = D_0\Delta t/(2a)^2$$

and with

$$\psi_0 = \frac{1+p}{2} + \frac{2}{\pi^2}(1-p)\sum_{k=1}^{\infty}\frac{1-(-1)^k}{k^2}\exp(-\pi^2k^2t')$$

The relieved behavior of the apparent self-diffusion coefficient for liquids in Scots pine sapwood made it tempting to check if the data could be analyzed simply by fitting the self-diffusion coefficients to eq 19. The equation showed though to not be suitable for curve fitting. Setting a as the variable parameter for optimization resulted in convergence to $a = 0$ even for the simulated self-diffusion coefficients if a was not given an initial value equal to the true value. Trying to optimize p through fitting was also not successful, as the resulting p was dependent on the initiated value. In Figure 14 are plotted theoretical values from eq 19 with a set to 13 μm. For comparison with the experimental data, p was set to 1, 0, and -1, respectively.

As seen in Figure 14, the theoretical self-diffusion coefficients with p set to zero or one closely follow the same behavior. The values calculated from the case with absorbing walls, i.e., $p = -1$, has on the other hand a deviating behavior compared to the two other cases. The validity of the Padé-approximation approach was further tested by fitting the values calculated with eq 19 to eq 18. In the case of a reflecting wall ($p = 1$) and an equally reflecting and absorbing wall ($p = 0$), the resulting fit of eq 18 was successful. The sum of the squared deviations was very small in these cases similar to the fits of the experimental self-diffusion coefficients. Also, $(2D_0\theta)^{1/2}$ obtained through the curve fittings was 13 ($\pm$1) μm. Self-diffusion coefficients calculated with p set to -1 were, on the other hand, not very well fitted to eq 18. Any chemical exchange between the wall surface and the lumen liquid pool can, thus, be ignored

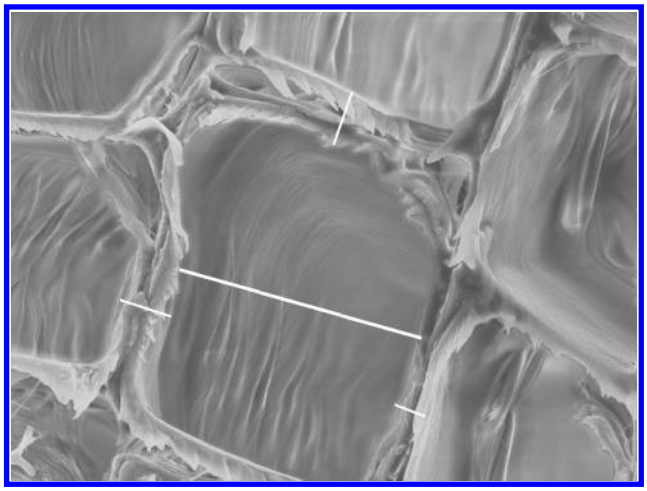

Figure 15. SEM image of earlywood tracheid cell cross section. The indicated lumen diameter of the cell is 30.8 μm, while the approximate wall thickness is 6 μm.

in the above structural interpretation of the experimentally observed self-diffusion coefficients. This was also the conclusion of D'Orazio and others.[24] In Figure 14, it is seen that at short diffusion times the observed self-diffusion coefficients are slightly lower than the theoretical values from diffusion between parallel planes. This is due to the fact that the cross section of the tracheid cells is not a perfect square. The cell corners may be rounded to varying degrees, and this would give a slightly stronger decrease in the observed self-diffusion coefficients at short diffusion times. The obtained surface-to-volume ratio will, though, be the same.[21]

The observed self-diffusion coefficients for both water and toluene fit very well to eq 18. The short diffusion time part of the behavior reveals the surface-to-volume ratio and, thereby, the cell side half length according to the geometrical definition of a square. The value of a is a bit different for the water experiments in comparison to the toluene experiments. The rates of the decays in the observed self-diffusion coefficients reveal the characteristic times, θ, which are very close for the two experiments. D_0 is for water 2.1×10^{-9} m^2 s^{-1} and for toluene 1.9×10^{-9} m^2 s^{-1}. Molecules from the two liquids thus experience the same part of the cell structure as the diffusion time proceeds. The characteristic lengths for diffusion in the cell matrix were calculated as $(2D_0\theta)^{1/2}$ with D_0 corresponding to either water or toluene. The characteristic length revealed from the water experiments was in perfect agreement with the cell side half length, a, calculated from the surface-to-volume ratio, while the toluene experiment gave a slight deviation between a and the characteristic length. Scanning electron microscopy (SEM) images of the wood sample revealed structural details of the tracheid cell matrix as shown in Figures 15 and 16.

Figure 15 shows a typical large cell from earlywood. Its lumen side half length was measured to 15.4 μm. Though the sample has been vacuum-dried, this value is representative for Scots pine earlywood.[2] In Figure 16 are shown all the cells in an annual ring. The earlywood with the largest cells is to the left. The cell lumen size decreases along the line toward the right, where it approaches zero as the wood turns to latewood. Along this line, 75 tracheid cells span the annual ring. The water PFG-NMR experiments gave a weighted average cell lumen side half length of 13 μm, and the largest cell lumen side half length is 15 μm, according to the SEM image. An estimation of the tracheid cell size distribution in an annual ring can then be done. When going from latewood to earlywood, the side half

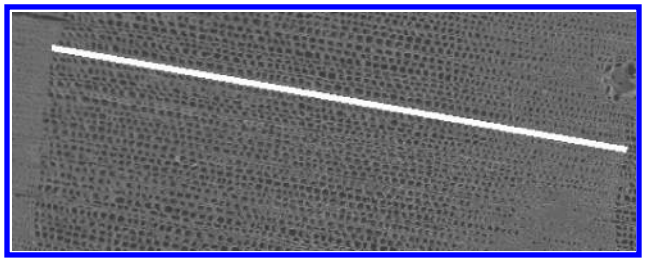

Figure 16. SEM image of an annual ring cross section. The width of this annual ring is 2280 μm. There are 75 tracheid cells spanning across the ring. This reveals an average cell diameter of 30.4 μm including the walls.

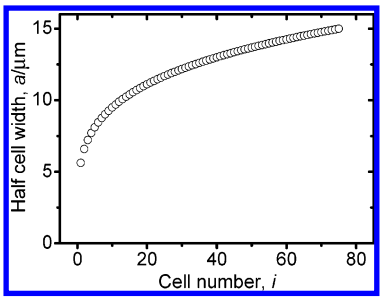

Figure 17. Tracheid cell lumen size in the annual ring with 75 cells, according to eq 24.

length of cell i can be set to

$$a_i = \beta i^{\alpha} \tag{20}$$

with $1 \le i \le 75$.

Two requirements are to be fulfilled for the distribution; the weighted cell side half length was given by the self-diffusion experiments, and the largest cell side half length was estimated from the SEM image:

$$\frac{\sum_{i=1}^{75} A_i a_i}{\sum_{i=1}^{75} A_i} = \frac{\sum_{i=1}^{75} a_i^3}{\sum_{i=1}^{75} a_i^2} = 13\,\mu\text{m} \tag{21}$$

$$\beta \cdot 75^{\alpha} = 15\,\mu\text{m} \tag{22}$$

where A_i is the cross-sectional area of cell i. Solving the latter equations for α and β and insertion into eq 20 gives the cell size distribution in the annual ring:

$$a_i = 5.6\,\mu\text{m} \cdot i^{0.23} \tag{23}$$

Applying eq 23 as a law for the cell lumen side half length distribution in an arbitrary annual ring in the wood sample, the cell lumen side half length is given as

$$a_i = 5.6\,\mu\text{m}\left(\frac{75i}{n}\right)^{0.23} \tag{24}$$

with $1 \le i \le n$ where n is the number of tracheid cells that span over the annual ring. Figure 17 is a plot of the above given cell side half length distribution in the sample annual ring.

Conclusion

It has been shown from principles of diffusion that self-diffusion coefficients of liquids confined in Scots pine sapwood can be used as a means of structure interpretation of the tracheid cellular matrix. The utilized PFG-NMR pulse sequence and low field NMR equipment give exponential echo attenuation curves and, thereby, average mean-square displacements and self-diffusion coefficients of liquids confined in cell lumens in the sample. Cross relaxation between the confined liquids and the wood tissue can be ignored with the applied pulse sequence, and the observed self-diffusion coefficients can be used in structure interpretation according to self-diffusion principles. The Padé approximant, which interpolates short and long diffusion time self-diffusion coefficients, converges quickly when fitting observed self-diffusion coefficients and is preferable compared to a analytic expression for diffusion between parallel walls. The organized and periodic structure of wood permits PFG-NMR self-diffusion measurements to be very well suited for nondestructive elucidation of the tracheid cellular structure of wood.

Acknowledgment. The Graduate School of Materials Research, Turku, Finland; the Nordic Research Board (NordForsk), Oslo, Norway; and the National Technology Agency in Finland (TEKES) are acknowledged for financial support. Mikael Järn, Turku, Finland, is thanked for help with the SEM images, and Olle Söderman, Lund, Sweden, is thanked for valuable discussions.

References and Notes

(1) Sen, P. N.; Basser, P. J. *Magn. Reson. Imaging* **2005**, *23*, 215.
(2) Jane, F. W. *The structure of wood*, 2nd ed.; Adam & Charles Black: London, 1970.
(3) Topgaard, D.; Soderman, O. *Biophys. J.* **2002**, *83*, 3596.
(4) Newling, B.; Batchelor, S. N. *J. Phys. Chem. B* **2003**, *107*, 12391.
(5) Price, W. S.; Barzykin, A. V.; Hayamizu, K.; Tachiya, M. *Biophys. J.* **1998**, *74*, 2259.
(6) Jiang, P. C.; Yu, T. Y.; Perng, W. C.; Hwang, L. P. *Biophys. J.* **2001**, *80*, 2493.
(7) Gaede, H. C.; Gawrisch, K. *Biophys. J.* **2004**, *86*, 30A.
(8) Gaede, H. C.; Gawrisch, K. *Biophys. J.* **2003**, *85*, 1734.
(9) Jäder, J. Dispersivitetens och syra-basväxelverkningarnas inverkan på vätskepenetreringen i träd. M.S. thesis, Kungliga Tekniska Högskolan, 1999.
(10) Larsson, A.; Stenius, P. *Nord. Pulp Pap. Res. J.* **1987**, *3*, 87.
(11) Törnqvist, M.; Hurme, T.; Rosenholm, J. B. *Pap. Puu* **2001**, *83*, 204.
(12) Dvinskikh, S. V.; Furo, I. *J. Magn. Reson.* **2000**, *146*, 283.
(13) Oleskevich, D. A.; Ghahramany, N.; Weglarz, W. P.; Peemoeller, H. *J. Magn. Reson., Ser. B* **1996**, *113*, 1.
(14) Soderman, O.; Jonsson, B. *J. Magn. Reson., Ser. A* **1995**, *117*, 94.
(15) Malmborg, C.; Topgaard, D.; Soderman, O. *J. Magn. Reson.* **2004**, *169*, 85.
(16) Fick, A. *Poggendorf's Ann. Phys. Chem.* **1855**, *170*, 59.
(17) Hagslatt, H.; Jonsson, B.; Nyden, M.; Soderman, O. *J. Magn. Reson.* **2003**, *161*, 138.
(18) Frey, S.; Kärger, J.; Pfeifer, H.; Walther, P. *J. Magn. Reson.* **1988**, *79*, 336.
(19) Einstein, A. *Ann. Phys.* **1905**, *17*, 549.
(20) Sen, P. N. *J. Phys.: Condens. Matter* **2004**, *16*, S5213.
(21) Mitra, P. P.; Sen, P. N.; Schwartz, L. M. *Phys. Rev. B* **1993**, *47*, 8565.
(22) Zimmermann, U.; Schneider, H.; Wegner, L. H.; Wagner, H.-J.; Szimtenings, M.; Haase, A.; Bentrup, F.-W. *Physiol. Plant.* **2002**, *114*, 327.
(23) Latour, L. L.; Mitra, P. P.; Kleinberg, R. L.; Sotak, C. H. *J. Magn. Reson., Ser. A* **1993**, *101*, 342.
(24) D'Orazio, F.; Bhattacharja, S.; Halperin, W. P.; Eguchi, K.; Mizusaki, T. *Phys. Rev. B* **1990**, *42*, 9810.